Holocene periodicity in North Atlantic climate and deep-ocean flow south of Iceland

Giancarlo G. Bianchi & I. Nicholas McCave

Department of Earth Sciences, University of Cambridge, Downing Street, Cambridge CB2 3EQ, UK

Climate fluctuations during the past millennium are relatively well documented[1]. On a longer timescale, there is growing evidence of millennial-scale variability of Holocene climate, at periodicities of ~2,500 and 950 years (possibly caused by changes in solar flux)[2,3] and ~1,500 years (maybe related to an internal oscillation of the climate system)[4–6]. But the involvement of deep water masses in these Holocene climate changes has yet to be established. Here we use sediment grain-size data from the Iceland basin to reconstruct past changes in the speed of deep-water flow. The study site is under the influence of Iceland–Scotland Overflow Water (ISOW), the flow of which is an important component of the 'thermohaline' circulation that modulates European climate. Flow changes coincide with some known climate events (the Little Ice Age and the Mediaeval Warm Period), and extend over the entire Holocene epoch with a quasi-periodicity of ~1,500 years. The grain-size data indicate a faster ISOW flow when the climate of northern Europe is warmer. However, a second mode of operation is observed in the early Holocene, when warm climate intervals are associated with slower ISOW flow. At that time the melting remnant of land-based, glacial-age ice may have provided a sufficient source of fresh water to the ocean to reduce ISOW flow south of Iceland.

The northeast Atlantic Ocean is of key importance for modulating climate on glacial–interglacial timescales because of heat loss to the atmosphere from the North Atlantic Current and its continuation through the Norwegian Sea, and the convective formation of deep water in the Nordic/Arctic seas, which together provide a temperate climate to northwestern Europe. The poleward flux of warm saline Atlantic waters is partly counterbalanced and maintained by the deep, dense, return flow of ISOW which crosses the Iceland–Scotland ridge mainly through the Faeroe Bank channel to enter the Iceland basin. Together with a similar dense overflow through the Denmark Strait, this process constitutes the initial step of the global ocean conveyor-belt model[7]. The thermohaline conveyor is unstable, and is sensitive to the fresh water/salt balance of the region[8]. Marine isotope stage 3 (~60–30 kyr before present, BP) was characterized by extreme millennial-scale climate instability, resulting in the Dansgaard–Oeschger temperature fluctuations seen in ice-core and marine records of temperature, and also resulting in ice rafting[9]. Our results show that even during the generally stable Holocene there is an underlying fluctuation in the strength of ISOW flow south of Iceland with a similar periodicity, which may be linked to climate changes.

The data we present have been obtained from kasten core NEAP-15K (56° 21.92′ N, 27° 48.68′ W) recovered from 2,848 m depth near the crest of Gardar drift in the south Iceland basin (see map in Fig. 1 inset). In this area Holocene sedimentation rates are greatly enhanced (Fig. 1b) owing to the interaction of bottom currents with the sea-bed topography, and the core contains a ~450-cm-long Holocene sediment record. We use a sedimentological near-bottom palaeocurrent speed proxy, the "sortable silt" mean size[10] ($\overline{SS}$ is the mean grain size of the 10–63-μm terrigenous silt fraction, a parameter that varies independently of sediment supply in current-sorted and deposited muds and for which higher values represent relatively greater near-bottom flow speeds). The mean Holocene deposition rate for the northeast Atlantic is ~4 cm kyr^{-1} (ref. 12). The core site is far from any sources of downslope mass transport, but is under the deep western boundary current of the Iceland basin which carries material from south Iceland and its continental slope[13] to create the ~1,100-km-long Gardar drift[14]. The very high sedimentation rates and particle sizes are thus primarily current-controlled, although fine sediment supply by ice rafting during the Holocene cannot be ruled out altogether. However, its effects would be negligible in core NEAP-15K as its Holocene accumulation rates for the terrigenous fine fraction (<63 μm) average ~20 g cm^{-1} kyr^{-1} with peaks of ~80 g cm^{-2} kyr^{-1}, whereas in full glacial conditions within the main ice-rafting belt just south of our site (at 51° 07.0′ N, 21° 52.0′ W) the flux from the sea surface for the same sediment component was only 1.5 g cm^{-2} kyr^{-1} (ref. 15). The accelerator mass spectrometry (AMS) ^{14}C dates used for the age model in Fig. 1c have been converted to calendar years BP[16] (where 'present' is AD 1950) after applying a 400-year reservoir correction. High-resolution dating was also successfully employed to splice the topmost part of NEAP-15K, which overpenetrated by 35 cm and scrambled the upper sediment section, with box core NEAP-16B recovered from the same site, thereby extending the record to the present day. Sedimentation rates (Fig. 1b) are fairly

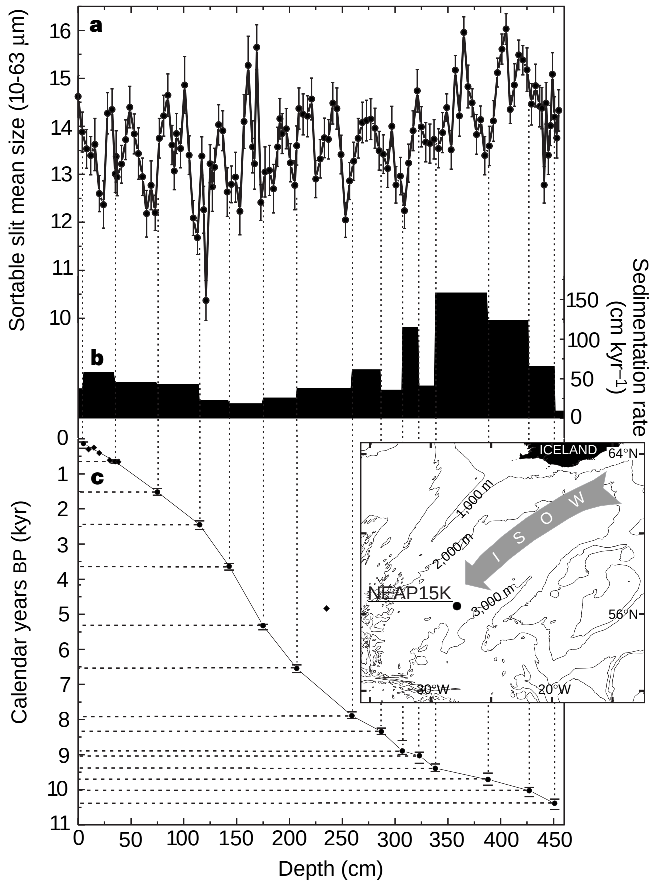

Figure 1 Data from kasten core NEAP-15K with an inset map showing its location in the south Iceland basin and the simplified regional flow of ISOW. **a**, Sortable silt mean size with error bars after ref. 18. **b**, Sedimentation rates between calendar years coinciding with ^{14}C AMS data used in age model. **c**, Filled circles represent ^{14}C AMS dates used to construct the age model, and filled diamonds are dates not included in the age model which were predominantly used to splice the uppermost part of NEAP-15K with the bottom of box core NEAP-16B. All dates are from monospecific assemblages of the planktonic foraminifera species *Globigerina bulloides* in the >150-μm fraction. The error range for the calendar dates is represented by horizontal bars above and below the solid circles and is defined as 2 standard deviations.

constant from 9.4 kyr ago to the present, but are significantly higher between ~10.4 and 9.4 kyr BP (~70–160 cm kyr^{-1}) due to the mobilization of sediments accumulated in glacial times by renewed ISOW flow[17]. The $\overline{SS}$ varies over the range ~10.5 to 16 μm (Fig. 2b), implying that sediment-sorting currents of significantly varying magnitude characterized the Holocene history of ISOW flow. We also note that a number of the fluctuations are small (~2 μm peak–trough but, nevertheless, significantly bigger than the precision of the method[18]), suggesting that some of the changes were subtle, probably reflecting the overall stable nature of sedimentation over the past 10,000 years.

The documented history of climate change in northern Europe over the past few millennia is marked by the alternation of cooler and warmer periods. At present we are still recovering from a time of colder climate known as the Little Ice Age[19], centred at ~400 yr BP, which, in our record, coincides with reduced ISOW flow intensity (Fig. 2b). The $\overline{SS}$ shows that since then, deep-water flow vigour has been increasing. Modern values are comparable to the last warm interval in European history, known as the Mediaeval Warm Period, which peaked at different times in various regions surrounding the North Atlantic basin between ~750 and 1,050 yr BP (AD ~900 to 1250)[1,20]. The climatic history in the few millennia before the Mediaeval Warm Period is less clear, but Europe appears to have enjoyed a warmer spell at ~2,000 yr BP, also referred to as the Roman Warm Period, followed by cooling and glacier advance in the Dark Ages (AD ~500 to 1000)[1,2]. In our record, a peak in deep-current speed centred at 1,850 yr BP (AD 100) coincides with the Roman Warm Period. From these observations and the flow speed fluctuations revealed by Fig. 2b we infer that periods comparable to the Little Ice Age and the Mediaeval Warm Period were a recurrent feature of earlier parts of Holocene climatic history, with the warm intervals coinciding with faster near-bottom water flow in the south Iceland basin.

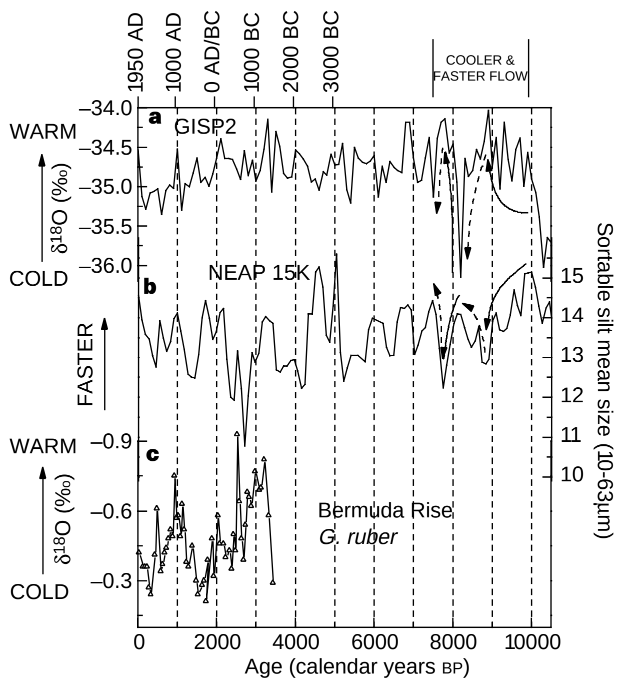

Figure 2 North Atlantic Holocene palaeoenvironmental proxy records on a calendar years BP (and AD/BC) basis. **a**, $\delta^{18}O$ data from central Greenland GISP2 ice core with gaussian interpolation using a 300-yr window. Solid and dashed arrows between ~10 and 7.5 kyr BP represent periods of general warming or cooling which match relative decreases or increases in the flow intensity of ISOW vigour (**b**), respectively. **b**, Sortable silt mean size record for NEAP-15K with gaussian interpolation using a 300-yr window. **c**, Planktonic foraminiferal $\delta^{18}O$ data from the Sargasso Sea (ref. 26), which mainly reflects changes in sea surface temperature.

The Holocene $\delta^{18}O$ record in the GISP2 Greenland ice core, which is thought to reflect mainly palaeotemperature changes[21], reaches typical Holocene values shortly after 10 kyr BP (Fig. 2a). From that time until ~7.5 kyr BP the broad temperature trends of the ice core are similar to our $\overline{SS}$ results (Fig. 2b), with intervals of lower temperatures over Greenland coinciding with times of more vigorous ISOW flow (we note the cycle between 8.9 and 7.5 kyr BP). After ~7.5 kyr BP, no clear or consistent relationship exists between the two (note that the faster flow during the cold "8.2 kyr event"[22] is well constrained within the 2σ range of dated points in Fig. 1a, c). We suggest that, because sea level was rising at a sustained rate until and just beyond 7.5 kyr BP[23], the flux of melt water to the northern North Atlantic must have been greater during warmer times; this would have had the effect of reducing the density and hence slowing down the flow of ISOW in the Iceland basin. The system flipped into its present state after ~7.5 kyr BP, when most of the remaining glacial ice had been melted and changes in temperature did not cause significant variations in the freshwater budget of the North Atlantic region.

The $\overline{SS}$ record was spectrally analysed (Fig. 3) following gaussian interpolation in the time domain using a 300-yr window and a 90-yr sampling interval (Fig. 2b). Only one broad but pronounced spectral density peak centred at 1,500 yr was obtained. This frequency of fluctuations in the intensity of ISOW flow is very similar to that of ice-rafting events recently reported for the past ~30,000 yr in the northeast Atlantic centred at 1,470 yr (ref. 4), to that of precipitation in western Canada[5], and to that of monsoon-related aridity/humidity cycles in Arabian dust (which have a 1,450–1,470-yr period[6]); it is also similar to one of the periodicities recorded in the sea surface and deep-water geochemical and faunal data from the Feni drift between 500 and 340 kyr BP[24]; and, finally, it is comparable with the 1,450-yr period present in the GISP2 ice-core chemical data produced by variation in wind strength and storminess due to changing atmospheric circulation patterns over the past 110 kyr (ref. 25). Our results therefore lend strong support to the idea that, as in glacial times[7], deep-water masses originating in the high-latitude North Atlantic play an important role in modulating climate in the present interglacial.

We also observe several similarities in the fluctuations between the $\overline{SS}$ record and a high-resolution history of surface-water foraminiferal $\delta^{18}O$ in the Sargasso Sea[26] for the past 3.5 kyr (Fig. 2b, c). The correlation, which shows $\delta^{18}O$ minima (warm) coinciding with periods of faster ISOW flow and vice versa, is $r = 0.47$ for the past ~1,500 yr and 0.76 for the past ~1,200 yr after introducing a lead of 90 yr to the $\overline{SS}$ data (this is acceptable as it is

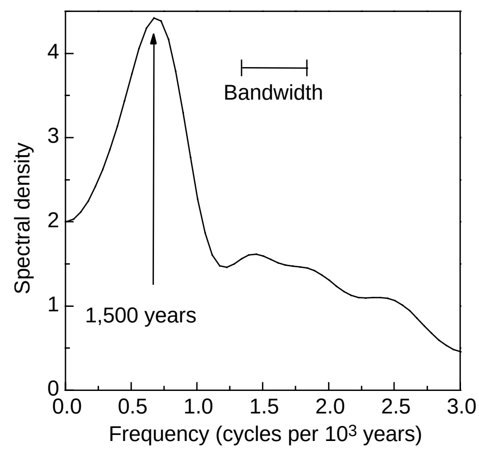

Figure 3 Spectral analysis by the Blackman-Tukey technique[34] of the sortable silt mean size record from NEAP-15K using data as shown in Fig. 2b. The 1,500-yr peak accounts for 26% of the total signal in the range above the Nyquist frequency (1/180 yr^{-1}) analysed (including red noise).

still within the errors of the dating techniques employed). Modern oceanographic studies show that, on decadal timescales under the influence of the North Atlantic Oscillation (NAO), convective overturning in the Sargasso and Greenland seas are linked[27]. However, we cannot explain in the same terms the apparent connection between these two regions on much longer, millennial timescales because the available evidence suggests that varying deep-water convection in the modern Greenland Sea does not affect the intensity of the overflows south of the Greenland–Scotland ridge[28]. The present 1990s extreme of the NAO has only slight convection in the Greenland–Norwegian seas area, but no diminution in the overflows[27,29]. This may be because a large component of ISOW volume flux is thought to originate from the North Atlantic Current entering the Arctic via cooling in the Barents Sea, and returning through Fram Strait, without any significant interaction with the Greenland gyre[30]. Larger-scale atmospheric feedbacks and reorganizations must be invoked to explain the connections observed between the surface northwest Atlantic and the flow intensity of ISOW, particularly in view of the pervasive ~1,500-yr periodicity we observe in our data and which is found in a variety of other proxies from the North Atlantic region[4,5,25] (in glacial as well as interglacial times) and from as far away as the Arabian Sea[6].

There is now no doubt that the Earth's climate is highly unstable on millennial timescales. However, our data do not provide an explanation for the ultimate forcing mechanism(s) of these events, and more than one process could be responsible for the changes in ISOW flow vigour recorded in core NEAP-15K. The speed of the overflow south of Iceland could be controlled by the influence of changes in either the salt- or freshwater flux on convection in the Nordic seas; alternatively, a shift in the density of shallow and intermediate water masses entrained by ISOW after overflowing the Iceland–Scotland ridge could also be responsible for the fluctuations of Fig. 2b[31]. Despite the problems in identifying the exact origin of the ISOW flow signal, our data shed light on both the sensitivity and the various operational modes of the thermohaline current system. In an initial early Holocene mode, freshwater flux from the land-based ice melted by warmer conditions is argued to be associated with reduced deep-water activity[32], resulting in a less dense and more sluggish ISOW flow over Gardar drift. Then, for the past 7.5 kyr, higher temperatures are in phase with more vigorous deep-water flow, under conditions similar to those at present with little melt water and an oscillation of the supply (by the North Atlantic Current) of saline water and heat to the Nordic seas. So far, no clear 1,500-yr periodicity in either ^{14}C or ^{10}Be has been reported from ice cores, suggesting that solar variation is an unlikely forcing mechanism and that an oceanic internal oscillation in 'conveyor' strength is more probable.

The main concern for future climate must be that a possible increase in melting of the Greenland ice sheet resulting from anthropogenically induced atmospheric warming may reach a critical level where the 'conveyor belt' will flip to its early Holocene operational mode[33]. The resulting perturbations could conceivably result in climate extremes exceeding those of the Little Ice Age for northern Europe. Without such perturbations, the climate looks likely to be warm for several hundred years (ref. 6). □

Received 29 June; accepted 7 December 1998.

1. Lamb, H. H. *Climatic History and the Future* (Princeton Univ. Press, 1985).
2. Röthlisberger, F. *10,000 Jahre Gletschergeschichte der Erde* (Sauerländer, Aarau, 1986).
3. O'Brien, S. R. *et al.* Complexity of Holocene climate as reconstructed from a Greenland ice core. *Science* **270,** 1962–1964 (1995).
4. Bond, G. *et al.* A pervasive millennial-scale cycle in North Atlantic Holocene and glacial climates. *Science* **278,** 1257–1266 (1997).
5. Campbell, I. D., Campbell, C., Apps, M. J., Rutter, M. W. & Bush, A. B. G. Late Holocene ~1500 year climatic periodicities and their implications. *Geology* **26,** 471–473 (1998).
6. Sirocko, F., Garbe-Schonberg, D., McIntyre A. & Molfino, B. Teleconnections between the subtropical monsoons and high-latitude climates during the last deglaciation. *Science* **272,** 526–529 (1996).
7. Broecker, W. S. & Denton, G. H. The role of the ocean-atmosphere reorganizations in glacial cycles. *Geochim. Cosmochim. Acta* **53,** 2465–2501 (1989).
8. Broecker, W. S., Bond, G. & Klas, M. A salt oscillator in the glacial Atlantic? 1. The concept. *Paleoceanography* **5,** 469–477 (1990).
9. Rasmussen, T. L., Thomsen, E., van Weering, T. C. E. & Labeyrie, L. Rapid changes in surface and deep water conditions at the Faeroe Margin during the last 58,000 years. *Paleoceanography* **11,** 757–771 (1996).
10. McCave, I. N., Manighetti, B. & Robinson, S. G. Sortable silt and fine sediment size/composition slicing: parameters for palaeocurrent speed and palaeoceanography. *Paleoceanography* **10,** 593–610 (1995).
11. McCave, I. N., Manighetti, B. & Beveridge, N. A. S. Circulation in the glacial North Atlantic inferred from grain-size measurements. *Nature* **374,** 149–152 (1995).
12. Balsam, W. L. & McCoy, F. W. Atlantis sediments: glacial/interglacial comparisons. *Paleoceanography* **2,** 531–542 (1987).
13. Shor, A. N. Bottom currents and abyssal sedimentation processes south of Iceland. Thesis, Woods Hole Oceanographic Inst. (1980).
14. McCave, I. N. & Tucholke, B. E. in *The Western North Atlantic Region* Vol. M (eds Vogt, P. R. & Tucholke, B. E.) 451–468 (Geol. Soc. Am., Boulder, 1986).
15. Manighetti, B. & McCave, I. N. Depositional fluxes, palaeoproductivity, and ice rafting in the NE Atlantic over the past 30 ka. *Paleoceanography* **10,** 579–592 (1995).
16. Stuiver, M. & Reimer, P. J. Extended ^{14}Ca data-base and revised calib 3.0 C-14 age calibration program. *Radiocarbon* **35,** 215–230 (1993).
17. Keigwin, L. D. & Jones, G. A. Glacial-Holocene stratigraphy, chronology, and paleoceanographic observations on some North Atlantic sediment drifts. *Deep-Sea Res.* **36,** 845–867 (1989).
18. Bianchi, G. G., Hall, I. N., McCave, I. N. & Joseph, L. Measurement of the sortable silt current speed proxy using the Sedigraph 5100 and Coulter Counter IIe: Precision and accuracy. *Sedimentology* (in the press).
19. Grove, J. M. *The Little Ice Age* (Methuen, London, 1988).
20. Grove, J. M. & Switsur, V. R. Glacial geological evidence for the Medieval Warm Period. *Clim. Change* **26,** 143–169 (1994).
21. Jouzel, J. *et al.* Validity of the temperature reconstruction from water isotopes in ice cores. *J. Geophys. Res.* **102,** 26471–26488 (1997).
22. Alley, R. B. *et al.* Holocene climatic instability: A prominent, widespread event 8,200 yr ago. *Geology* **25,** 483–486 (1997).
23. Bard, E. *et al.* Deglacial sea-level record from Tahiti corals and the timing of global meltwater discharge. *Nature* **382,** 241–244 (1996).
24. Oppo, D. W., McManus, J. F. & Cullen, J. L. Abrupt climate events 500,000 to 340,000 years ago: evidence from subpolar North Atlantic sediments. *Science* **279,** 1335–1338 (1998).
25. Mayewski, P. A. *et al.* Major features and forcing of high-latitude northern hemisphere atmospheric circulation using a 110,000-year-long glaciochemical series. *J. Geophys. Res.* **102,** 26345–26366 (1997).
26. Keigwin, L. D. The Little Ice Age and Medieval Warm Period in the Sargasso Sea. *Science* **274,** 1504–1508 (1996).
27. Dickson, R. R., Lazier, J., Meincke, J., Rhines, P. & Swift, J. Long-term coordinated changes in the convective activity of the North Atlantic. *Prog. Oceanogr.* **38,** 241–295 (1996).
28. Dickson, R. R. & Brown, J. The production of North Atlantic Deep Water: Sources, rates and pathways. *J. Geophys. Res.* **99,** 12319–12341 (1994).
29. van Aken, H. M. & Becker, G. Hydrography and through-flow in the north-eastern North Atlantic Ocean: the NANSEN project. *Prog. Oceanogr.* **38,** 297–346 (1996).
30. Mauritzen, C. Production of dense overflow waters feeding the North Atlantic across the Greenland-Scotland Ridge. Part 1: Evidence for a revised circulation scheme. *Deep-Sea Res. I* **43,** 769–806 (1996).
31. Price, J. F. & Baringer, M. O'N. Outflows and deep water production by marginal seas. *Prog. Oceanogr.* **33,** 161–200 (1994).
32. Sakai, K. & Peltier, W. R. A multibasin model of the global thermohaline circulation: Paleoceanographic analyses of the origins of ice-age climate variability. *J. Geophys. Res.* **101,** 22535–22562 (1996).
33. Broecker, W. S. Thermohaline circulation, the Achilles heel of our climate system: Will man-made CO_2 upset the current balance? *Science* **278,** 1582–1588 (1997).
34. *OS-3 ARAND SYSTEM: Documentation and Examples* Vol. 1 (Computer Center, Oregon State Univ., 1973).

Acknowledgements. We thank S. Crowhurst for help in the spectral analysis of the data presented here, N. Shackleton for comments on an earlier draft, and R. Dickson for hydrographic observations. This work was supported by UK NERC for the North East Atlantic Palaeoceanography and Climate Change project (NEAPACC).

Correspondence and requests for materials should be addressed to G.G.B. (e-mail: ggb20@esc.cam.ac.uk).

Auditory distance perception in rooms

Adelbert W. Bronkhorst & Tammo Houtgast

TNO Human Factors Research Institute, PO Box 23, 3769 ZG Soesterberg, The Netherlands

The perceived distance of a sound source in a room has been shown to depend on the ratio of the energies of direct and reflected sound[1]. Although this relationship was verified in later studies[2–4], the research has never led to a quantitative model. The advent of techniques for the generation of virtual sound sources[5,6] has made it possible to study distance perception using controlled, deterministic stimuli. Here we present two experiments that make use of such stimuli and we show that a simple model, based on a modified direct-to-reverberant energy ratio, can accurately predict the results and also provide an explanation for the 'auditory horizon' in distance perception. The modification of the ratio consists of the use of an integration time of 6 milliseconds in the